

Transition from laminar to vortical current flow in electron waveguides with circular bends

K.-F. Berggren* and Zhen-Li Ji

Department of Physics and Measurement Technology, Linköping University, S-581 83 Linköping, Sweden

(Received 10 August 1992; revised manuscript received 12 October 1992)

We have analyzed the spatial flow pattern in two-dimensional ballistic electron waveguides with circular bends. For a double bend the conductance may still be perfectly quantized in spite of the strong mixing of modes. In narrow energy regions just below the subband thresholds there is strong interference between localized and propagating solutions, causing an interference blockade. Within these regions the current flow becomes vortical. Minor changes in, e.g., energy cause drastic changes in the flow pattern.

I. INTRODUCTION

Currently there is much interest in the electron movement in ultrasmall structures such as dots, rings, wires, and other narrow constrictions. Structures of this kind may be achieved in modulation-doped semiconductor heterojunctions, e.g., GaAs-Al_xGa_{1-x}As, in which the electrons are initially confined at the interface in the form of a two-dimensional (2D) electron gas. Precision lithography is used to tailor the 2D gas into the desired pattern. This makes it possible to investigate electron transport in the ballistic regime where the mean free path of the electrons exceeds the size of the device. If the Fermi wavelength λ_F is comparable to the dimensions of the very small structure quantization effects become important. Recent reviews of this very active and rapidly increasing field are found in Refs. 1 and 2.

Here we will consider narrow conducting channels or wires having bends. If λ_F is comparable to the width transverse motion will play an important role and it is appropriate to view the wire as an electron waveguide with distinct modes or subbands. In a very narrow waveguide only a few of these modes would be occupied. In a real device the modal occupancy may be altered by applying different gate and/or substrate voltages or by means of magnetic depopulation. Another important feature due to the wave nature of the electrons is that bends in a waveguide, in general, give rise to bound states or evanescent waves. For applications it is of interest to understand various aspects of electron transport in narrow wires. They may, for example, be integrated into waveguide circuits and serve as fast transmission leads in ultrasmall, close-packed devices. One must then have a good general understanding of the influence of bends. As we wish to show below bends also give rise to physical phenomena which are interesting from a more fundamental point of view. We will then assume that there is no scattering from impurities and that interaction effects are less effective. In this sense the transport is ballistic.

In recent years there has been a number of explicit calculations³⁻⁷ as well as more formal proofs⁸ showing that a system consisting of an infinite quantum wire with a single circular bend has a square-integrable bound state below the lowest subband threshold. Such an elementary structure is thus able to trap a particle. In addition

there are anomalies associated with higher subband thresholds. Instead of perfectly bound states one then finds quasibound states or evanescent waves in a very narrow energy window just below the mode propagation thresholds. These states interfere destructively with the normal, propagating modes. As a result the transport in a particular mode becomes entirely blocked in a narrow range of energies, i.e., there is an interference blockade. This is similar to the scattering in a quantum wire with, e.g., a weak attractive scatter⁹ or a local widening,¹⁰ which also gives rise to sharp dips in the conductance. Another nontrivial theoretical result for the infinite wire with a circular bend is that the conductance G can be quantized to a very high precision in the regions of energy in between the quasibound states, i.e., $G = 2e^2N/h$ where N is the modal occupancy. The quantization occurs in spite of the very strong mode mixing that sets in as the Fermi energy E_F is increased above the first subthreshold state.^{3,4,6}

The properties of an electron waveguide with circular bends is also remarkable from the following point of view. As we will show here the current flow is laminar in regions of energy in which the conductance is well quantized. However, at the subthreshold energies at which an interference blockade occurs the current swiftly becomes vortical with quite a complex texture. This would imply that if E_F is gradually increased a current flow that is initially laminar would turn into a vortical one as soon as E_F comes into the very vicinity of a quasibound state, but on further increase of E_F the laminar flow would be restored until the next quasibound state is reached and so on. In this respect a quantum wire with bends stands out as a unique model system. In spite of its elementary features this system thus displays an intriguing physics of principle interest.

At a first glance the transition from laminar to vortical flow is reminiscent of the behavior of classical fluids and gases. However, hydrodynamic vortices in such media occur because of forces between particles or volume elements. Hence the formation of vortices in our one-electron waveguide system appears to have no hydrodynamics analogue as the phenomenon is entirely due to wave-mechanical interference. Classical waveguides therefore appear to be more natural analogues, in particular, two-dimensional planar waveguide circuits.¹¹

Scattering parameters for various planar structures designed for filtering¹² purposes indeed display strong dips reminding of the interference blockade in the bent electron waveguide discussed above. In general, however, it appears that little attention is given to the corresponding spatial distributions of currents, etc., in classical waveguide structures. In fact, the quantum-mechanical case has also received relatively little attention which may seem a bit surprising in view of the tremendous interest in recent years in ballistic transport in quantum wires, lateral superlattices, rings, etc.^{1,2} Some work has, however, started to appear in the literature. Thus the transmission through a quantum box or resonator has been shown to give rise to vortex excitations related to resonances.^{13–16} Current distributions around elastic scatterers and arrays of dots and antidots have also been calculated, without^{17,18} and with a perpendicular magnetic field.^{19,20} Although a different type of system one may also mention the curly, turbulent-looking eddy quantum current that has been obtained in model calculations of the tunnel current in a scanning tunneling microscope.^{21,22}

II. ELECTRON STATES AND TRANSPORT IN AN IDEAL WIRE WITH CIRCULAR BENDS

To calculate the one-electron states and current flow in an ideal quantum wire with two circular bends with radius R we assume a simple model similar to that of Refs. 3–6. We start by letting the wire be infinitely long, i.e., we do not bother with the details of how electrons are injected into the wire or emitted from it. This case has recently been treated also in Ref. 23, but with a different focus. Thus the electrons are confined by a hard-wall potential to the wire of constant width d (see Fig. 1). Within the wire the 2D Hamiltonian for the single electron of effective mass m^* is written as

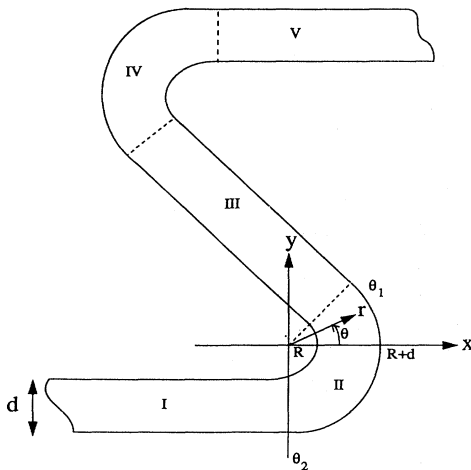


FIG. 1. Schematic of the waveguide having two circular bends with the same bending angle ($\Theta_1 + \Theta_2$). The constant width is d and the inner radius is R . Electrons are assumed to be injected into the subband from the far left. Sections I–V are used in the expansion of the wave functions.

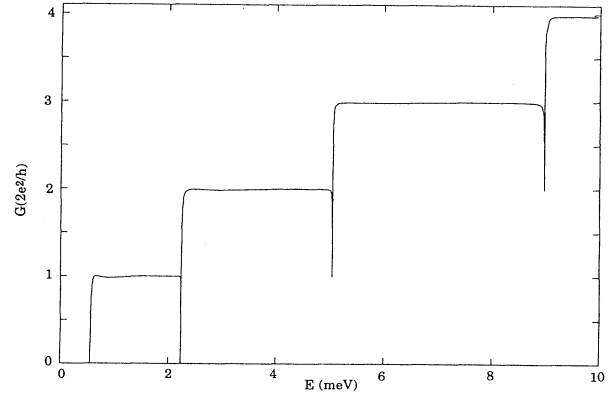


FIG. 2. Zero-temperature conductance G in units of $(2e^2/h)$ (total transmittance) in a waveguide with two 90° circular bends ($\Theta_1 = 0$ and $\Theta_2 = \pi/2$). The width is $d = 100$ nm and the inner radius $R = 10$ nm. The length of Sec. III is 2 nm. Eight modes are included in the calculation of G .

$$(\Delta + k^2)\Psi(x, y) = 0, \quad (1)$$

where $k^2 = 2m^*E/\hbar^2$. Because of the hard walls the wave function Ψ must vanish at the boundaries. The solutions in the straight secs. I, III, and V are elementary. For an electron injected from the left into the n th mode one has

$$\Psi_{I,n}(x, y) = e^{iq_n x} \sin \left[\frac{n\pi}{d}(y + R) \right] + \sum_m r_{nm} e^{-iq_m x} \sin \left[\frac{m\pi}{d}(y + R) \right], \quad (2)$$

where the coefficients r_{nm} give the probability amplitudes for reflection. If $E > E_m$, where E_m is the transverse threshold energy $E_m = \hbar^2(m\pi/d)^2/2m^*$, the momentum

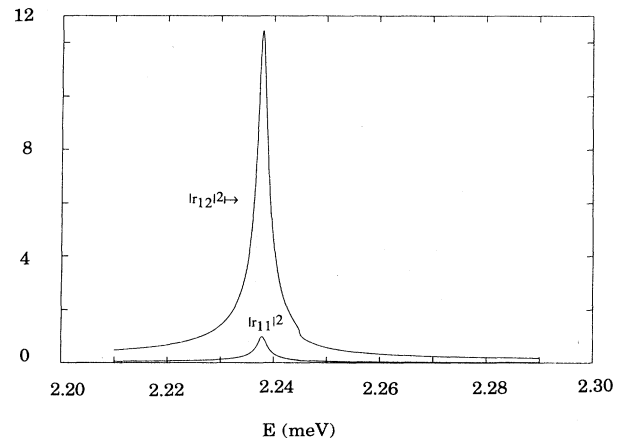


FIG. 3. Wave-function coefficients r_{11} and r_{12} vs energy at the first interference blockade just below the second subband threshold (seen as the small edge on the high-energy side of $|r_{12}|^2$). An incident electron in the lowest mode $n = 1$ may be completely backscattered, i.e., $|r_{11}|^2 \rightarrow 1$. The weight of the exponential component, $|r_{12}|^2$, is by far the dominant one, i.e., there is an “almost bound” or “quasibound” state.

of the corresponding propagating mode is $q_m = \{2m^*(E - E_m)\}^{1/2}/\hbar$. In the other case with $E < E_m$ the backscattered mode turns into the exponential solution $\exp(-|q_m|x)$, which decays in the correct way as $x \rightarrow -\infty$. The solution in region III is similar to Eq. (3) but the expansion of $\Psi_{\text{III},n}$ must contain all modes propagating forwards and backwards as well as both exponentially damped and increasing states. In region V only outgoing propagating modes are retained, i.e.,

$$\Psi_{V,n}(x, y') = \sum_m t_{nm} e^{iq_m x} \sin\left(\frac{m\pi}{d}(y' + R)\right), \quad (3)$$

where t_{mn} gives the transmission probability; y' refers to a symmetrically shifted coordinate system. For $E < E_m$ the outgoing wave turns into the decaying state $\exp(-|q_m|x)$.

Now consider the circular bend defining region II. Using polar coordinates $\mathbf{r} = (r, \Theta)$ one may construct a wave function that is qualitatively very similar to the wave functions above, i.e.,

$$\Psi_{\text{II},n} = \sum_j (a_{nj} e^{ip_j \Theta} + b_{nj} e^{-ip_j \Theta}) \Phi_{p_j}(r), \quad (4)$$

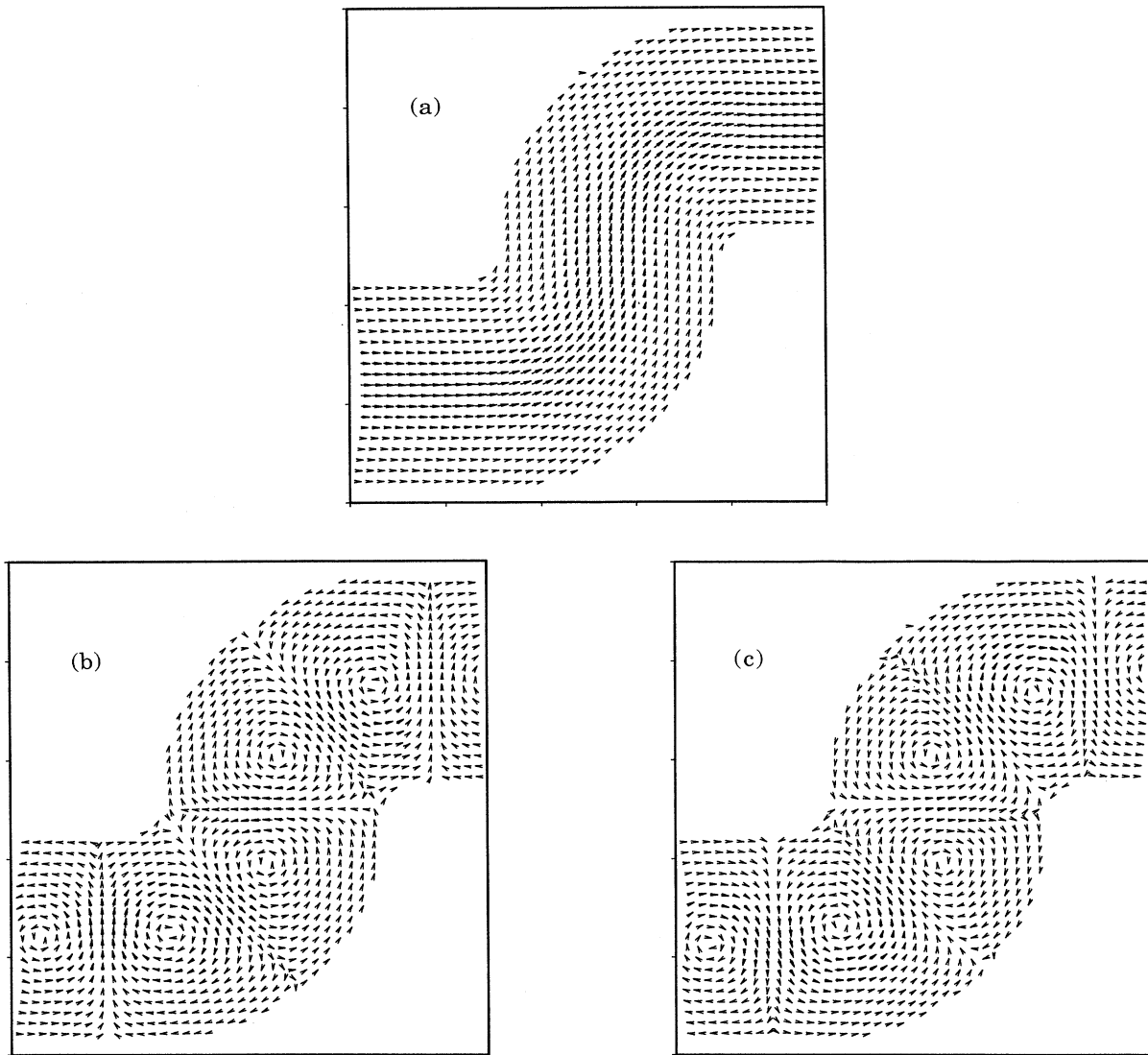


FIG. 4. Spatial probability distribution of the velocity \mathbf{v}_{op} corresponding to Fig. 2. Case (a) shows the laminar flow in the first subband for the energy $E_F = 1.5$ meV and a precisely quantized conduction. Larger arrows mean higher velocities. Case (b) shows the formation of vortices at the first conduction dip just below the second subband threshold. E_F is immediately to the left of the conductance minimum and $G \approx 0.2(2e^2/h)$. In case (c) E_F is immediately to the right of the interference minimum and $G \approx 0.8(2e^2/h)$. The minute change in energy has induced a swift reversal of the vortices reminiscent of spin flips.

where the exponentials correspond to the propagating modes above and $\phi_{p_j}(r)$ to the transverse mode; a_{n_j} and b_{n_j} are expansion coefficients to be determined. Since the system is azimuthally asymmetric and the circular bends are connected to external leads the p_j need not be integers. In fact, p_j will be either real or purely imaginary implying propagating or exponentially damped/increasing states, respectively.

To solve for $\Phi_{p_j}(r)$ and p_j we expand the solution in the basis set $\chi_l(r) = \sin[l\pi/d(r-R)]/\sqrt{r}$ with $l=1,2,\dots$. With expansion coefficients $a_l(p_j)$. We chose this basis because it appears naturally when the problem of a circular bend is approximately mapped onto a one-dimensional quantum well having bound states.⁵ Inserting the expansion in the Schrödinger equation, multiplying by $\chi_m(r)$ and integrating from R to $(R+d)$ one has

$$\sum_l \left[[k^2 - (l\pi/d)^2] \langle m|r^2|l \rangle - (p_j^2 - \frac{1}{4}) \frac{d}{2} \delta_{l,m} \right] a_l(p_j) = 0, \quad (5)$$

where $\langle m|r^2|l \rangle = \int dr r^2 \sin[m\pi/d(r-R)] \sin[l\pi/d(r-R)]$. The symmetric eigenvalue problem yields positive and negative real values for p_j^2 . A simple coordinate transformation gives the solutions appropriate to the second bend.

Expansion parameters r_{mn} , t_{mn} , etc., are obtained by matching wave-function amplitudes and derivatives at the various boundaries. The matching results in an inhomogeneous set of linear equations which is solved numerically. To determine the spatial probability distribution of velocities $\mathbf{v}(x,y)$ from these solutions, we assume that electrons are injected far from the left within a small range of energies ($E_F - eV, E_F$), where eV is the drop in potential energy. Then

$$\mathbf{v}(x,y) \propto \sum_n (\Psi_n^* \mathbf{v}_{\text{op}} \Psi / q_n) eV \Theta(E_F - E_n), \quad (6)$$

where \mathbf{v}_{op} is the velocity operator and $\Theta(E)$ a step function. The summation is over all incoming occupied modes n . The conductance G is obtained by integrating Eq. (6) over the transverse coordinate at the far end of the wire, i.e., there is the usual result

$$G = (2e^2/h) \sum_{n,m} [Re(q_m)/q_n] |t_{mn}|^2 \Theta(E_F - E_n). \quad (7)$$

To conclude the formal outline we recall that a bound state wave function is obtained by omitting the incoming wave in Eq. (2). If there is a bound state, its binding energy is determined by the condition that the corresponding homogeneous set of linear equations for the expansion coefficients has nontrivial solutions. Such a condition is used below.

III. NUMERICAL RESULTS

A. Conductance

Figure 2 shows the conductance in a waveguide with two 90° bends and with a short intermediate section. In all calculations we have set the effective mass m^*

$= 0.067m_0$ which is appropriate to GaAs-Al_xGa_{1-x}As. We have also assumed that the temperature is zero. As for a single bend^{4,6} the conductance is quantized to a high degree of accuracy in spite of very strong intermode scattering. Hence the situation is reminiscent of the recent modeling of Castaño and Kirzenow of the nonadiabatic, quantized transport in a smooth ballistic constriction.²⁴ Adiabaticity is not required for quantized conductance. Figure 2 also shows that the narrow conduction dips due to the quasibound states occurring just below the subband thresholds. For example, in the lowest mode $|r_{11}|^2$ and $|r_{12}|^2$ behave like very sharply peaked Lorentzians centered at the conduction minimum as shown in Fig. 3. The width of the Lorentzians and the dip is of the same order. At the interference blockade the backscattering becomes complete, i.e., $|r_{11}|^2 \rightarrow 1$. The weight of the exponential component, $|r_{12}|^2$, is by far the dominant one, i.e., the state is “almost bound” or “quasibound.” Below the first subband threshold this kind of state turns into very shallow, but truly bound state.²⁵ The binding energy increases with increasing bending angle. In general, one expects a pairwise splitting of both the bound and quasibound states in a double bend, but for more shallow states, as in Fig. 2, the upper ones are pushed into the adjacent subband continua. The effect of finite leads is similar. In fact, both dips in G associated with quasibound states and tunneling resonances for bound states may fade away for shorter leads. The extension of the middle Sec. III in Fig. 1 also affects the conductance. For very long intersections the splitting of the states becomes less pronounced. In addition there will be weak oscillations superimposed on the plateaus in G related to standing waves in the middle section.²³

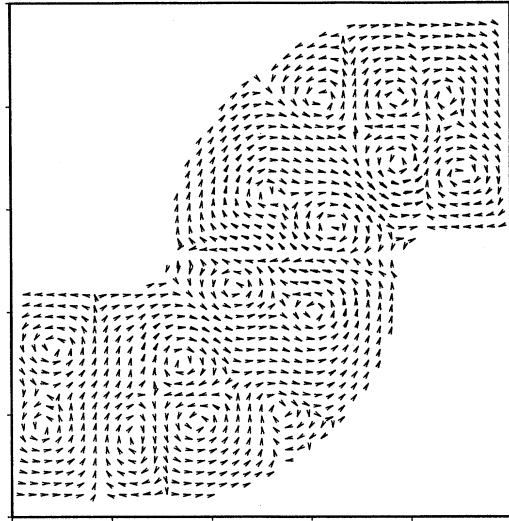


FIG. 5. Same as Fig. 3 but for E_F immediately to the left of the second conduction dip [$G \approx 1.4(2e^2/h)$]. Flow directions reverse in the same drastic way as in Fig. 4 as we move slightly to the right of the conduction minimum.

B. Spatial distributions of velocities

Figures 4(a)–4(c) and 5 constitute the real core of this paper. The message is quite striking and there is little need for additional comments. In case (a) the conduction is well quantized and the flow is perfectly laminar. In the very narrow energy window, where the interference blockade sets in, the initially laminar flow suddenly turns into violent vortices susceptible to drastic changes on minute changes of, e.g., the Fermi energy E_F . Cases (b) and (c) show how a clockwise flow suddenly reverses into anticlockwise motion and vice versa. Well into the second subband laminar flow is restored until the second interference dip is reached on further increase of E_F . Then vortical flow with an even richer pattern sets in as shown in Fig. 5. This picture is repeated periodically as we proceed to higher subbands.

In summary we have shown that an elementary one-electron model for an elementary electron waveguide

having circular bends predicts regions of laminar and vortical flow and rapid transitions between them. Transport anomalies associated with quantum interference are certainly well known, but little attention has been given to the complexity of the corresponding spatial flow patterns. Thus it is amazing and inspiring that a modeling as basic as the present one can still yield intriguing physics which is even of considerable aesthetic value. Although it appears that an experimental verification would be hard to achieve the results are of principal interest with bearings on quantum chaos and related phenomena.

ACKNOWLEDGMENTS

This work was supported in part by the Swedish Natural Science and Engineering Research Councils. One of us (K.-F.B.) would also like to thank Trinity College, Cambridge, UK, for support and M. Pepper for informative discussions.

*Also at Cavendish Laboratory, Cambridge, UK.

¹C. W. J. Beenakker and H. van Houten, in *Quantum Transport in Semiconductor Nanostructures*, edited by H. Ehrenreich and D. Turnbull, Solid State Physics Vol. 44 (Academic, New York, 1991).

²S. E. Ulloa, A. MacKinnon, E. Castaño, and G. Kirzenow, *From Ballistic Transport to Localization*, edited by P. T. Landsberg (North-Holland, Amsterdam, 1992), Vol. I.

³C. S. Lent, *Appl. Phys. Lett.* **56**, 2554 (1990).

⁴F. Sols and M. Macucci, *Phys. Rev. B* **41**, 11 887 (1990).

⁵D. W. L. Sprung, Hua Wu, and J. Martorell, *J. Appl. Phys.* **71**, 515 (1992).

⁶K. Vacek, H. Kasai, and A. Okiji, *J. Phys. Soc. Jpn.* **61**, 27 (1992).

⁷J. Goldstone and R. L. Jaffe, *Phys. Rev. B* **45**, 14 100 (1992).

⁸P. Exner and P. Seba, *J. Math. Phys.* **30**, 2574 (1989).

⁹P. F. Bagwell, *Phys. Rev. B* **41**, 10 354 (1990).

¹⁰T. Itoh, N. Sano, and A. Yoshii, *Phys. Rev. B* **45**, 14 131 (1992).

¹¹See, e.g., *Numerical Techniques for Microwave and Millimeter-Wave Passive Structures*, edited by T. Itoh (Wiley, New York, 1989).

¹²See, e.g., K. C. Gupta and M. D. Abouzahra, *Numerical Techniques for Microwave and Millimeter-Wave Passive Structures* (Ref. 11), Chap. 4.

¹³C. S. Lent, *Appl. Phys. Lett.* **57**, 1678 (1990).

¹⁴K.-F. Berggren, C. Besev, and Zhen-Li Ji, *Proceedings of the Nobel Jubilee Symposium, Low Dimensional Properties of Solids, Chalmers University of Technology, Gothenburg,*

Sweden, 1991 [Phys. Scr. **T42**, 141 (1992)].

¹⁵K.-F. Berggren, C. Besev, and Zhen-Li Ji, *Proceedings of the International Workshop on Quantum-Effect Physics, Electronics and Applications, Luxor, Egypt, 1992*, edited by K. Ismail, T. Ikoma, and H. I. Smith, IOP Conf. Proc. No. 127 (Institute of Physics and Physical Society, Bristol, 1992), p. 25.

¹⁶C. Besev, Zhen-Li Ji, and K.-F. Berggren, *Cray Channels* (Cray Research, Mendota Heights, Minnesota, 1992), Vol. 14, p. 20.

¹⁷Zhen-Li Ji and K.-F. Berggren, *Phys. Rev. B* **45**, 6652 (1992).

¹⁸Zhen-Li Ji, *Semicond. Sci. Technol.* **7**, 198 (1992).

¹⁹S. Chaudhuri, S. Bandyopadhyay, and M. Cahay, *Phys. Rev. B* **45**, 11 126 (1992); and unpublished.

²⁰M. Leng and C. S. Lent, *Superlatt. Microstruct.* **11**, 351 (1992).

²¹Th. Laloyaux, A. A. Lucas, J.-P. Vigneron, Ph. Lambin, and H. Morawitz, *J. Microsc.* **152**, 53 (1988).

²²A. A. Lucas, *Europhys. News* **21**, 63 (1990).

²³J. C. Wu, M. N. Wybourne, A. Weisshaar, and S. M. Goodnick (unpublished).

²⁴E. Castaño and G. Kirzenow, *Phys. Rev. B* **45**, 1514 (1992).

²⁵Bound states of this kind have recently been observed for microwave radiation in a similar geometry by J. P. Carini, J. T. Londergan, K. Mullen, and D. P. Murdock, *Phys. Rev. B* **46**, 15 538 (1992). Electrons in a serpentine superlattice may also be regarded as a somewhat related case, see, e.g., M. S. Miller, H. Weman, C. E. Pryor, M. Krisnamurty, P. M. Petroff, H. Kroemer, and J. L. Merz, *Phys. Rev. Lett.* **68**, 3464 (1992); Craig Prior, *Phys. Rev. B* **44**, 12 912 (1991).